Vieira, D. H., Badiei, N., Evans, J. E., Alves, N., Kettle, J. and Li, L. (2020) Improvement of the deep UV sensor performance of a β-Ga2O3 photodiode by coupling of two planar diodes. *IEEE Transactions on Electron Devices*, 67(11), pp. 4947-4952. (doi: 10.1109/TED.2020.3022341)

The material cannot be used for any other purpose without further permission of the publisher and is for private use only.

There may be differences between this version and the published version. You are advised to consult the publisher's version if you wish to cite from it.

http://eprints.gla.ac.uk/225739/

Deposited on 02 November 2020

Enlighten – Research publications by members of the University of Glasgow
http://eprints.gla.ac.uk

Improvement of the deep UV sensor performance of a β-Ga_2O_3 photodiode by coupling of two planar diodes

D. H. Vieira, N. Badiei, J. E. Evans, N. Alves, J. Kettle, L. Li

Abstract — β-Ga_2O_3 is one of promising semiconductor materials that has been widely used in power electronics and ultraviolet (UV) detectors due to its wide bandgap and high sensitivity to UV light. Specifically, for the UV detection application, it has been reported that the photocurrent was in the scale of micro Amps (μA), which normally requires sophisticated signal processing units. In this work, a novel approach based upon coupling of two Schottky diodes has been designed, which demonstrates a much higher photocurrent in the mA range (~186 times higher than the classic Schottky diode design). The detectivity and responsivity of the new device have also been significantly increased. The rectification ratio of this device was measured to be 1.7 x 10^7 with ultra-low dark current, when measured in the reverse bias. Those results confirm the approach of coupling two Schottky diodes has great potential in high performance deep UV sensor applications.

***Index Terms* — Gallium Oxide, Photodetector, Deep UV, Schottky Diode, Performance Improvement.**

I. INTRODUCTION

OVER the past 5 years, significant international efforts have been conducted on new forms of ultraviolet (UV) photodiodes for a wide range of applications such as in the military, environmental, medical and industrial markets which require the sensor to operate in harsh situations [1]. The most common commercial UV photodiodes are Si-based, but these possess limited sensitivity at UV wavelengths [2]. Wide bandgap semiconductor materials, such as MgZnO and AlGaN, had been reported as an alternative to Si, but it remains a challenge to achieve good crystalline quality as a result of the heavy doping levels needed [3]. Gallium oxide (Ga_2O_3) stands out as an alternative material to UV photodiodes and has been the subject of intense recent research [4]. It can be manufactured with five crystallographic phases: α, β, γ, δ and ε, although the β phase (β-Ga_2O_3) has been the most used in electronic devices applications due to its chemical and thermodynamic stability [5]. Furthermore, β-Ga_2O_3 has a very large breakdown field (E_b) value and a wide bandgap, ~8 MV/cm and 4.9 eV [6], respectively. It is a promising material for power electronics and its ability to handle high electrical fields is greatly advantageous for the reduction of device size and enhancement of the integration level of power modules [7]. Aiming to explore these advantageous properties, many devices have been reported using this material as the active layer, for example: Schottky diodes [8], transistors [9], solar cells [10], gas sensors [5] and LEDs [11]. Most significantly, β-Ga_2O_3 is also an ideal candidate for deep UV sensing applications such as for solar-blinds [12] because it eliminates the need to use interference filters [13] and achieves high values of rejection ratio of visible light [14,15]. This material also can be applied to biomedical area, detection of corona discharge, UV curing of paints/adhesives, machine vision, monitoring UV exposure for skin cancer, forensics, flame and chemical sensing [16].

One of the biggest challenges for manufacturing β-Ga_2O_3 devices is to achieve a robust ohmic contact. This difficulty arises from the β-Ga_2O_3 surface due to the upward band bending

The work was supported by the Solar Photovoltaic Academic Research Consortium II (SPARC II) project, gratefully funded by WEFO.

J. Kettle is with the School of Electronic Engineering, Bangor University - Bangor, Wales, UK. (e-mail: j.kettle@bangor.ac.uk).

N. Badiei, J. E. Evans and L. Li, are with the Multidisciplinary Nanotechnology Centre, College of Engineering, Swansea University, Swansea, Wales, UK. (e-mail: n.badiei@swansea.ac.uk, j.e.evans@swansea.ac.uk and l.li@swansea.ac.uk, respectively).

D. H. Vieira and N. Alves are with the Departamento de Física, UNESP - São Paulo State University, Presidente Prudente, Brazil. (e-mail: douglas.vieira@unesp.br and neri.alves@unesp.br, respectively).

inducing electron depletion [17]. Yao *et al* reported Ti, In, Ag, Sn, W, Mo, Sc, Zn and Zr [18] as materials suitable for ohmic contact. Higashiwaki *et al* reported the first β-Ga_2O_3 transistor using Ti/Au as an ohmic contact [6], but to achieve this condition it was necessary to use reactive ion etching (RIE) with a mixture of BCl_3 and Ar. Bae *et al* reported that this same Ti/Au contact also can be rectifier [19]. The later states that contact properties depend on the atmosphere in which the material is annealed because it is highly dominated by the formation of oxygen vacancies. The barrier height also seems to be affected by the interface states and impurities [7]. It has been showed that moderate annealing (~400 ºC) improves the Ti/Au ohmic behavior [18] and also tends to yield higher ideality factors in diodes [20], that is related to the high barrier, but Carey *et al* reported that Ti/Au (20nm/80nm) can presents high resistance Schottky behavior even if annealed at 300, 400, 500 and 600 ºC [21]. The mixture of ohmic and Schottky contacts with the same material on the Ga_2O_3 devices may give rise to novel UV detecting devices with much improved performances. It was reported that the photocurrent of Ga_2O_3 based UV detectors have been small (µA range) [15], which is probably attributed to the fact that achieving highly conductive Ga_2O_3 is challenging to manufacture.

In this work, we report the performance of a β-Ga_2O_3 Schottky diode in a planar architecture using Ti/Au as electrode for the ohmic and Schottky contact. This device showed promising properties both as a diode and as a deep UV photodetector. However, we are able to dramatically improve the performance (photocurrent) by inclusion of a third Ti/Au electrode, resulting in a two-diode coupled device. The influence of voltage bias at this third electrode was studied and the device exhibited substantial enhancement of all figures of merit of photodetectors in comparison to the Schottky diode.

II. EXPERIMENTAL DETAILS

β-Ga_2O_3 (010) wafer with thickness of 0.5 mm and face polishing obtained by edge-defined film-fed growth (EFG) method was purchased from Tamura Corporation®. The substrate was grown with Sn as dopant at a concentration of $8.3x10^{18}$ cm^{-3}. The substrate was thoroughly cleaned using acetone, isopropanol and dried with nitrogen followed by placing them 10 minutes on 150 °C hotplate for complete dehydration. The contacts were patterned via a lift-off process. Samples were spin coated with 2 % PMMA 950K (EM Resists Ltd.) at 3000 rpm, exposed using electron beam lithography (EBL) at an acceleration voltage of 30 kV then developed using 1:3 MIBK:IPA. To form the electrical contacts, a 20 nm Ti layer followed by a 100 nm Au layer were deposited on the surface of β-Ga_2O_3 wafer using physical vapor deposition (PVD). **Fig. 1a** shows a picture of the device. After the electrode deposition, the sample was submitted to a rapid thermal annealing (RTA) at 400 ºC for 1 min in a N_2 atmosphere at a pressure of approximately 1 mbar. Although all the contacts pads were prepared on the sample concurrently, they do not all have the same characteristics; some are measured as Schottky and others as ohmic, due to the gradient of distribution of interface states and impurities at the film surface, which is a common problem in β-Ga_2O_3 devices.

Two types of devices were studied: 1) two-terminal devices, i.e a Schottky diode and 2) three-terminal device formed by the coupling of two Schottky diodes. The cross-section of both devises are presented at the **Fig 1b**, identifying which contacts are ohmic and which contacts are Schottky. The chosen pads design for the Schottky diode and for the photodetector form a planar structure with an active area of 0.02048 cm². An Agilent B2912A unit connected to a probe station was used to obtain current versus voltage (I–V) and current versus time (I–t) curves using it in the dark and deep UV (254 nm, 1.58 mW/cm^2), at room temperature and atmosphere. To calculate the photodetector figures of merit (FOM), the power density of the UV light was measured using a UV-enhanced photodiode purchased from Thorlabs (model FDS010).

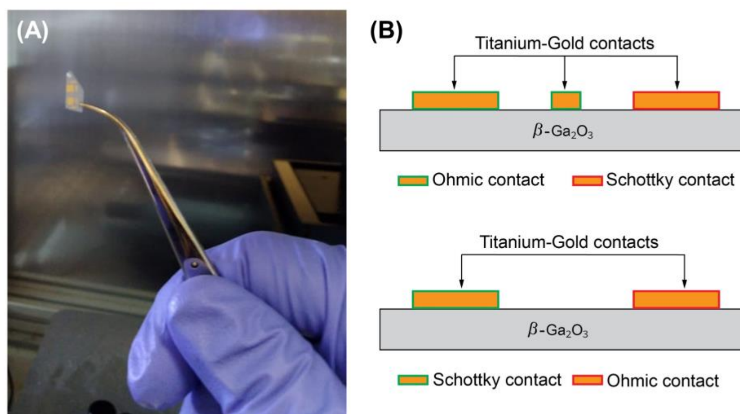

Fig 1. a) Photograph of the β-Ga_2O_3 device and b) cross sectional diagram showing the cross-section of the β-Ga_2O_3 devices of te coupled Schottky diode (top) and conventional Schottky diode (below)

III. RESULTS AND DISCUSSION

A. Results of Schottky diode experiments

Fig. 2a presents the I−V characteristics of the β-Ga$_2$O$_3$ Schottky diode in the dark and under UV irradiation. In the dark, this curve presents a typical rectification behavior expected for Schottky diodes by the following equation:

$$I = AA^{*}T^{2} \exp\left(-\frac{q\phi_B}{kT}\right)\left[\exp\left(\frac{qV_d}{nkT}\right) - 1\right] \quad (1)$$

where q is electron charge, ϕ_B is Schottky barrier height, V_d is applied voltage, k is Boltzmann constant, T is temperature, n is ideality factor, A is effective area and A^* is effective Richardson constant. This β-Ga$_2$O$_3$ Schottky diode exhibited good rectifying properties with a high rectification ratio of ($RR = I_{forward}/I_{reverse}$) $9.16x10^6$ between ± 10 V, a forward turn-on voltage of around 2 V and also a low current under reverse bias (~10^{-11} A). The series resistance (R_s) was calculated as 9.6 $k\Omega$ using the Cheung's method ($R_s = \frac{dV}{dlnI}\frac{q}{nkT}$) [22]; the large R_s is syntomic by the non-ideal Ti/β-Ga$_2$O$_3$ contact.

Under UV exposure (254 nm, 1.58 mW/cm^2), the photodiode exhibits a significant change in the current under reverse bias (see **Fig. 2**). To evaluate the performance of this device as a deep UV photodetector, figures of merit were calculated, in particular: responsivity (R_λ), external quantum efficiency (EQE), detectivity (D^*) and PDCR (photo to dark current ratio). The responsivity and EQE were estimated using equations 2 and 3, respectively:

$$R_\lambda = \frac{J_{ph}}{P_d}, \quad (2)$$

$$EQE(\%) = \frac{R_\lambda hc}{q\lambda} x100, \quad (3)$$

with J_{ph} being the photocurrent density, P_d the power density of the incident light, h the Planck's constant, c the speed of light and λ the exciting wavelength. The calculated values of responsivity and EQE were 0.0125 A/W and 6.12 %, respectively. Detectivity and PCDR were used to characterize the response of our sensors and were calculated using equations 4 and 5, respectively. Consequently, the calculated detectivity and PDCR of the Schottky diode was measured at 1.02x10^{12} Jones and 4.26x10^4, respectively.

$$D^* = \frac{R_\lambda}{\sqrt{2qJ_{dk}}}, \quad (4)$$

$$PDCR = \frac{I_{uv} - I_{dk}}{I_{dk}}, \quad (5)$$

From the results above, this diode exhibits sensing behaviour for deep UV detection, but it presents a poor responsivity, when compared to state-of-the-art performances in the literature. The likely reason for this is the poorer quality a β-Ga$_2$O$_3$ formed as a result of the PVD process used in this work, which could be overcome by using the more established epitaxially grown processes.

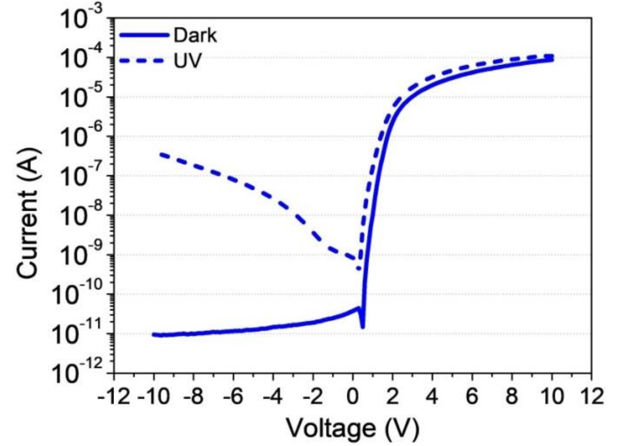

Fig. 2: I-V curves of the β-Ga$_2$O$_3$ Schottky diode in the dark and under UV light.

In the context of the next section, it is important to understand the physical mechanism for the generation of photocurrent in this device. Around the proximity of the Schottky contact in β-Ga$_2$O$_3$ devices, there are traps due to oxygen deficiency and, under deep UV exposure, the photogenerated pair disassociates, leading to the holes being trapped in the oxygen vacancies, preventing recombination with the electrons and increasing the depletion layer [23]. These mechanisms can be represented by the follow equation, where UV is the incident photon and V_o is an oxygen vacancy:

$$UV + V_o^0 \rightarrow V_o^{2+} + 2e^-. \quad (6)$$

The change in the charge concentration near the Schottky contact increases the internal electric field and lowers the effective Schottky barrier in the reverse bias, thus leading to an increase in the current [13]. Using the Cheung's method, it was calculated a lowing effect of 0.2 eV (the barrier changed from 0.94 eV in the dark to 0.74 eV under UV light).

B. Results of coupled Schottky diode experiments

In order to improve performance and achieve higher FOM values, the device was modified by coupling to a third Schottky electrode. In the inset of **Fig. 3a,** a schematic equivalent circuit is presented of this novel configuration. **Fig. 3a** shows the I−V characteristics of the coupled Schottky diode in dark, where the voltage level of the third electrode (V_{third}) is modified from 0 V to 9 V. Those curves continue to show a typical rectification behavior expected for a Schottky diode and it also presents a high current of 2 mA in the forward bias. Moreover, when different levels of the third voltage was applied, it was possible to adjust the turn-on voltage, from around 2 V to around 7 V, although all curves reach approximately the same maximum current due to limitations in the bulk limited region. **Fig. 3b**

shows that the turn-on voltage has a linear relationship with the voltage level at the third electrode.

Fig. 3c shows the I−V characteristics of the coupled Schottky diode in the dark and under deep UV (254 nm, 1.58 mW/cm^2) for different voltage biases at the third electrode (from 0 V to 9 V). In the dark, this device has low current in reverse bias and reaches milliamps in forward voltage bias, evidenced by the high rectification ratio of $1.76x10^7$ at $\pm$ 10 V and 9 V at the third electrode. This rectification ratio does not change significantly in the dark, even when varying voltages biases are applied at the third electrode. Furthermore, this increase in the level at the third electrode does not affect significantly the current in the reverse bias in the dark.

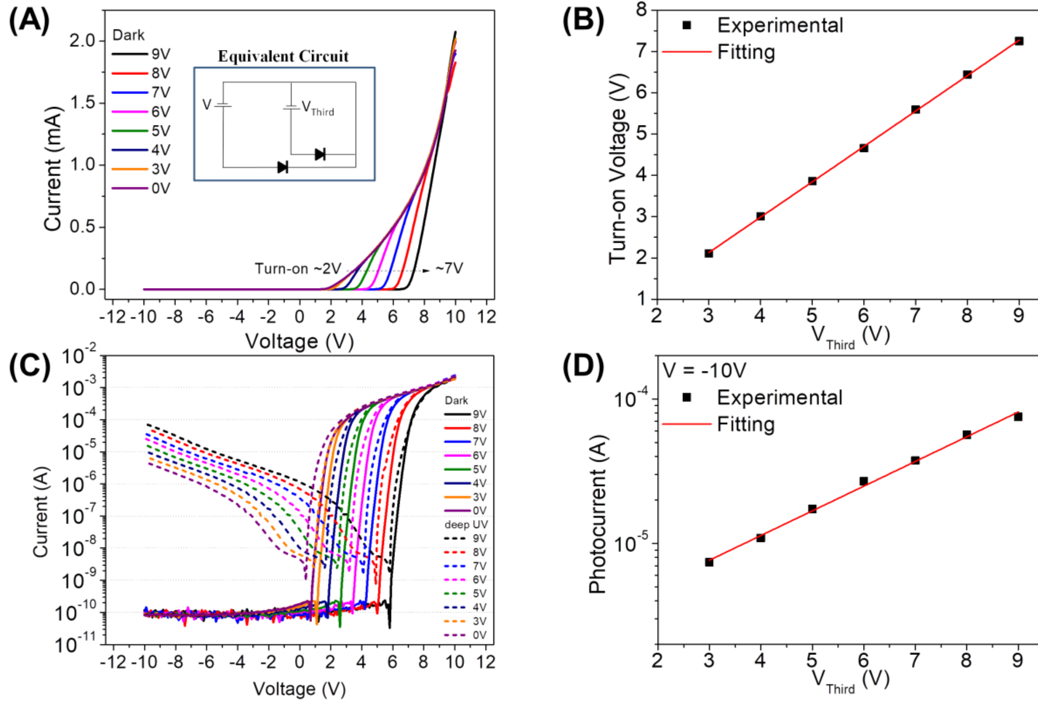

Fig. 3: a) I-V characteristics of the coupled Schottky diode in the dark under varying voltage biases at the third electrode with (inset) equivalent circuit of the coupled diode. b) Turn-on voltage versus voltage appied at the third electrode at V = −10 V. c) I - V characteristics of the coupled Schottky diode in the dark and under UV irradaiton at different voltage biases at the third eletrode. (d) Photocurrent versus third electrode voltage at V = −10V.

Under UV irradiation, it is evident that the photocurrent increases significantly in the reverse bias leading to higher photocurrents. **Fig. 3d** shows that the logarithmic value of the photocurrent has increases linearly with V_{Third}, i.e. the coupled Schottky diode leads to increase the photocurrent, resulting in a much higher value than can be achieved from a Schottky diode. The photocurrent ($I_{uv} - I_{dk}$) at 254 nm, $V_{Third} = 9\ V$ and $V = -10\ V$ was 75.3 µA, which is 186 times greater than the photocurrent observed in the single Schottky diode reported in **Fig. 2**.

The internal electric potential difference is impacted by the presence of the third electrode which seems to shift the diode bias by an amount equal to the change in On-voltage. This is supported by **Fig. 4**, which presents a 2D simulation of the electric potential profile for the coupled Schottky diode at reverse bias. The third electrode creates a potential gradient between the Schottky and third electrode leading increased electron-hole pairs formation in this region. Thus, a higher voltage bias applied to the third electrode corresponds to greater efficiency in charge collection and, consequently, greater photocurrent.

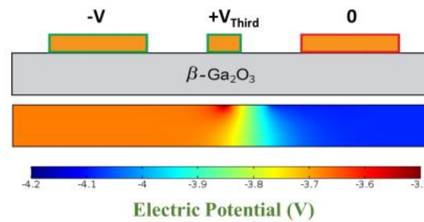

Fig. 4: 2D simulation of the electric potential profile for a coupled Schottky diode at reverse bias."

To evaluate the photoresponse, measurements were made in order to obtain the rise and decay time constants. **Fig. 5a** shows the current as a function of time measurements (*I*-*t*) for the coupled Schottky diode, with $V = -10\ V$, in the dark and under illumination, varying the level at the third electrode. To obtain the rise time constant, curves were fitted using by the following equation under UV light exposure:

$$I(t) = I_o + Ae^{-t/\tau_r}, \qquad (7)$$

where I_o and A are constants, t is the time, and τ_r is the rise time constant.

At $V_{third} = 0\,V$, the rise time was found as 70.50 s. However, when the level at the third electrode was changed, not only the photocurrent increases, but also it was possible to achieve better rise times, with the fitted value for rise time being measured as 29.38 s at $V_{third} = 9\,V$. **Fig. 5b** summarizes the differences in the rise time and photocurrent as a function of the bias on V_{Third}; with the highest value of $V_{third}(9\,V)$, it is possible to achieve the shortest rise time constant and highest photocurrent, as highlighted in red. This change in time constant is related to the change in the internal potential as illustrated in **Fig. 4**. When the electron-hole pair is formed by the incident deep UV irradiation and it is dissociated, those charges are accelerated by this potential resulting in a shift that increases with the voltage level.

After the UV light is switched off, the current as a function of time (I-t) changes to a bi-exponential relationship. Likewise, the decay time constant was obtained for each curve, after turned-off the UV source, can be modeled using the following equation [24]:

$$I(t) = I_o + Ae^{-(t-t_o)/\tau_{d1}} + Be^{-(t-t_o)/\tau_{d2}}, \quad (8)$$

where B and t_o are constants, τ_{d1} and τ_{d2} are the first and second decay time constant, respectively.

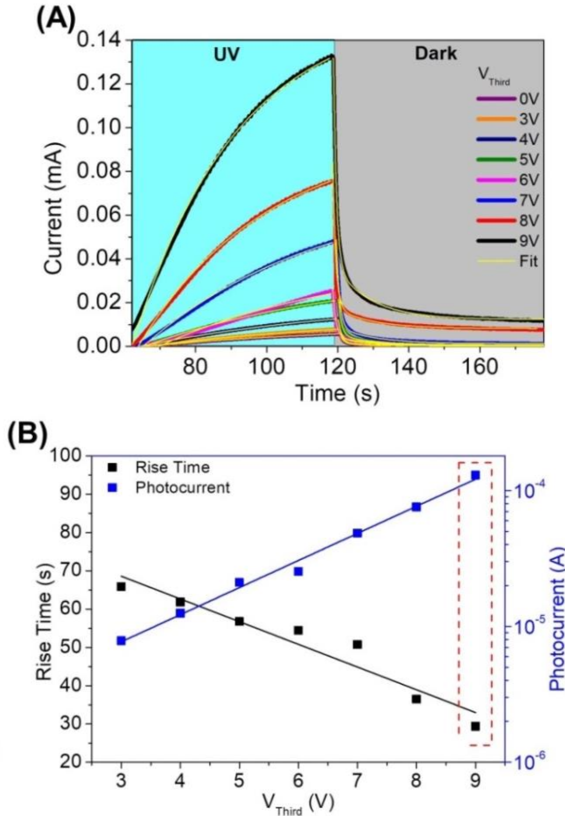

Fig 5: a) Rise and decay curves for photocurrent (I – t) of the coupled Schottky diode in the dark and under UV for different voltages bias at the third eletrode, and b) Rise time and photocurrent versus voltage at the third electrode.

The first decay time constant (τ_{d1}) was found to be 0.86 s, which probably relates to the recombination of the electrons formed in the conduction band with the holes from recombination centers present in the material, or from a band-to-band annihilation process [25]. The second time constant (τ_{d2}) was found to be 10.17 s, which is a much slower component and can be attributed to deep traps [25] that generates a persistent photocurrent effect [26]. Both rise and decay times do not change with the applied voltage at the third electrode.

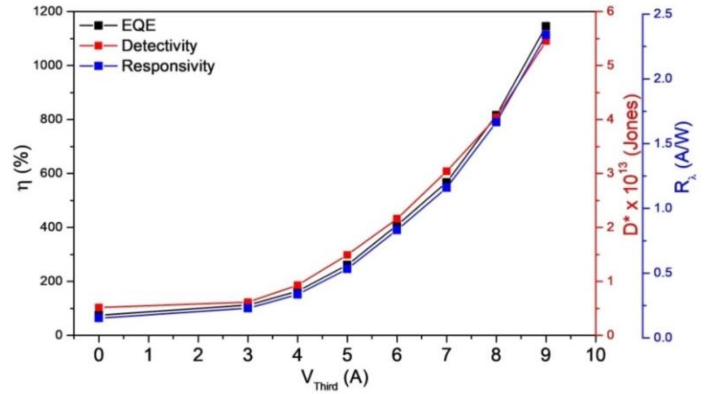

Fig. 6: Responsivity, external quantum efficiency (EQE/(η) and detectivity as a function of third electrode voltage (V_{Third}) for the coupled Schottky diodes.

Overall, the coupled Schottky diodes showed an enhanced in the photodetector figures of merit. The responsivity and EQE of the simple Schottky diode have presented 0.0125 A/W and 6.12 %, respectively. By the insertion of the third electrode with $V_{third} = 0\,V$ bias, those values increased to 0.153 A/W and 74.88 %, respectively. However, by applying a greater voltage bias at the third electrode, the potential is enhanced increasing the photocurrent generation leading to higher values of both parameters, with maximum of 2.34 A/W and 1145.24% at $V_{third} = 9$ V, respectively. More than 100% in EQE can be achieved if the internal gain increases with the voltage [27]. It can be related to changes in the depletion layer at the junction [28].

Fig. 6 shows the responsivity, EQE and detectivity as a function of the voltage bias on the third electrode. In terms of the detectivity, the simple Schottky diode has achieved a value of $1.02\text{x}10^{12}$ Jones that was improved to $5.18\text{x}10^{12}$ Jones for the coupled diode with $V_{third} = 0\,V$, which increased to $5.45\text{x}10^{13}$ Jones at $V_{third} = 9\,V$. The PDCR of the simple Schottky diode was obtained as $4.26\text{x}10^4$ at 254 nm, that was improved to $6.09\text{x}10^4$ for the coupled diode with $V_{Third} = 0\,V$ and $V = -10\,V$ and increased to $6.38x10^5$ when $V_{Third} = 9\,V$, which is a high light/dark ratio and represents an increase of one order of magnitude compared to the simple Schottky diode. The dark current has a negligible change during UV exposure from 10^{-11} to 10^{-10} A, which provides an attractive noise floor that is competitive with almost all UV detectors [24].

TABLE I:
COMPARISON OF THE PARAMETERS TO EVALUATE THE PERFORMANCE OF THE DEVICE AS DEEP UV PHOTODETECTOR WITH DIFFERENT VOLTAGE BIAS AT THE THIRD ELECTRODE.

	Simple Schottky diode	Coupled diode with $V_{Third} = 0\,V$	Coupled diode with $V_{Third} = 9\,V$
Responsivity (A/W)	0.0125	0.153	2.34
EQE (%)	6.12	74.88	1145.24
Detectivity (Jones)	1.02×10^{12}	5.18×10^{12}	5.45×10^{13}
PDCR	4.26×10^{4}	6.09×10^{4}	6.38×10^{5}
I_{dk} reverse bias (A)	1.0×10^{-11}	8.1×10^{-11}	1.1×10^{-10}

311 Finally, we summarize the performance differences of the 312 Schottky diode versus the coupled Schottky diode. **Tab I** 313 provide a direct comparison of the control device (Schottky 314 diode) versus the novel coupled-diode device reported in this 315 paper. It is clear that the best performance is achieved using the 316 coupled-diode device, in particular when the third terminal is 317 biased to the highest possible voltage (in our case this was tested 318 to $V_{Third} = 9\,V$). When comparing to the state of the art, 319 Nakagomi *et al* [29] reported a diode with extremely low rise 320 and decay time, but it responsivity was 0.053 A/W, which is 321 better than our simple Schottky diode, but with the coupled 322 Schottky diodes, we achieve a responsivity of 2.34 A/W. Kong 323 *et al* [30] reported a high responsivity of 39.3 A/W, but it rise 324 time was 95 s which compares unfavorably to our results 325 29.38 s. The FOMs that are most prominently above the state of 326 the art are the PDCR and dark current reinforcing the fact that 327 the coupling of two diodes is a promising result for deep UV 328 sensor applications. Further studies should be conducted upon 329 the coupled devices to measure the responsivity as a function of 330 wavelength; this might lead to higher responsivity values than 331 those reported in this manuscript
332

333 ## IV. CONCLUSION

334 The work reports the UV sensing behaviour of a β-Ga_2O_3- 335 based coupled Schottky diode. This device exhibited good 336 properties as rectification ratio, low dark current in reverse bias 337 and a high forward current of 2 mA. The use of three terminals 338 device instead of the conventional two terminals simple 339 Schottky diode enables a substantial improvement in 340 performance. The diodes shown high PDCR and good values of 341 responsivity, EQE and detectivity. From the results, we confirm 342 that this novel configuration of a coupled Schottky diode has 343 enormous potential for deep UV sensor applications.
344

345 ## ACKNOWLEDGMENTS

346 The work was supported by the Solar Photovoltaic Academic 347 Research Consortium II (SPARC II) project, gratefully funded 348 by WEFO. The authors thank the Fundação de Amparo à 349 Pesquisa do Estado de São Paulo (FAPESP) (Grant No. 350 2019/14366-3) and Programa de Pós-Graduação em Ciência e 351 Tecnologia de Materiais (POSMAT) for technical and financial 352 support.
353

354 ## REFERENCES

355 1. Nakagomi, S., Momo, T., Takahashi, S. & Kokubun, Y. Deep 356 ultraviolet photodiodes based on β-Ga2O3/SiC heterojunction. *Appl.* 357 *Phys. Lett.* **103,** (2013).
358 2. Qin, Y. *et al.* Review of deep ultraviolet photodetector based on 359 gallium oxide. *Chinese Phys. B* **28,** (2019).
360 3. Yu, J. *et al.* Influence of annealing temperature on structure and 361 photoelectrical performance of beta-Ga2O3/4H-SiC heterojunction 362 photodetectors. *J. Alloys Compd.* **798,** 458–466 (2019).
363 4. Pratiyush, A. S., Xia, Z., Kumar, S., Zhang, Y. & Joishi, C. MBE-364 Grown β-Ga2O3-Based Schottky UV-C Photodetectors With 365 Rectification Ratio ~10^7. *IEEE Photonics Technol. Lett.* **30,** 2025–366 2028 (2018).
367 5. Pandeeswari, R. & Jeyaprakash, B. G. High sensing response of β-368 Ga2O3 thin film towards ammonia vapours: Influencing factors at 369 room temperature. *Sensors Actuators B Chem.* **195,** 206–214 (2014).
370 6. Higashiwaki, M., Sasaki, K., Kuramata, A., Masui, T. & Shigenobu, 371 Y. Gallium oxide (Ga2O3) metal-semiconductor field-effect 372 transistors on single-crystal β-Ga2O3 (010) substrates. *Appl. Phys.* 373 *Lett.* **100,** (2012).
374 7. Huiwen, X. *et al.* An Overview of the Ultrawide Bandgap Ga2O3 375 Semiconductor-Based Schottky Barrier Diode for Power Electronics 376 Application. *Nanoscale Res. Lett.* (2018).
377 8. Li, A. *et al.* Investigation of temperature dependent electrical 378 characteristics on Au/Ni/β-Ga2O3 Schottky diodes. *Superlattices* 379 *Microstruct.* (2018). doi:10.1016/j.spmi.2018.04.045
380 9. Thomas, S. R. *et al.* High electron mobility thin-film transistors 381 based on Ga2O3 grown by atmospheric ultrasonic spray pyrolysis at 382 low temperatures. *Appl. Phys. Lett.* **105,** (2014).
383 10. Minami, T., Nishi, Y. & Miyata, T. Effect of the thin Ga2O3 layer 384 in n+-ZnO/n-Ga2O3/p-Cu2O heterojunction solar cells. *Thin Solid* 385 *Films* **549,** 65–69 (2013).
386 11. Vasanthi, V., Kottaisamy, M., Anitha, K. & Ramakrishnan, V. Near 387 UV excitable warm white light emitting Zn doped γ-Ga2O3 388 nanoparticles for phosphor-converted White Light Emitting Diode. 389 *Ceram. Int.* (2018). doi:10.1016/j.ceramint.2018.10.111
390 12. Guo, X. C. *et al.* β-Ga2O3/p-Si heterojunction solar-blind ultraviolet 391 photodetector with enhanced photoelectric responsivity. *J. Alloys* 392 *Compd.* **660,** 136–140 (2016).
393 13. Oshima, T. *et al.* β-Ga2O3-based metal-oxide-semiconductor 394 photodiodes with HfO2 as oxide. *Appl. Phys. Express* **11,** 1–4 395 (2018).
396 14. Oh, S., Kim, C. K. & Kim, J. High Responsivity β-Ga2O3 Metal-397 Semiconductor-Metal Solar-Blind Photodetectors with Ultraviolet

Transparent Graphene Electrodes. *ACS Photonics* **5,** 1123–1128 (2018).

15. Liu, Z. *et al.* A high-performance ultraviolet solar-blind photodetector based on a β-Ga2O3 Schottky photodiode. *J. Mater. Chem. C* **7,** 13920–13929 (2019).
16. Pratiyush, A. S., Krishnamoorthy, S., Muralidharan, R., Rajan, S. & Nath, D. N. *Advances in Ga2O3 solar-blind UV photodetectors*. *Gallium Oxide: Technology, Devices and Applications* (Elsevier Inc., 2019). doi:10.1016/B978-0-12-814521-0.00016-6
17. Hou, C., Gazoni, R. M., Reeves, R. J. & Allen, M. W. Direct comparison of plain and oxidized metal Schottky contacts on β-Ga2O3. *Appl. Phys. Lett.* **114,** (2019).
18. Yao, Y. A. O., Davis, R. F. & Porter, L. M. Investigation of Different Metals as Ohmic Contacts to β-Ga2O3: Comparison and Analysis of Electrical Behavior, Morphology, and Other Physical Properties. *J. Electron. Mater.* (2016). doi:10.1007/s11664-016-5121-1
19. Bae, J., Kim, H.-Y. & Kim, J. Contacting mechanically exfoliated β-Ga2O3 nanobelts for (opto)electronic device applications. *ECS J. Solid State Sci. Technol.* **6,** Q3045–Q3048 (2017).
20. Lyle, L. A. M., Jiang, L., Das, K. K. & Porter, L. M. *Schottky contacts to β-Ga2O3*. *Gallium Oxide* (Elsevier Inc., 2019). doi:10.1016/B978-0-12-814521-0.00011-7
21. Carey, P. H. *et al.* Ohmic contacts on n-type β-Ga2O3 using AZO/Ti/Au. *AIP Adv.* **7,** 1–7 (2017).
22. Cheung, S. K. & Cheung, N. W. Extraction of Schottky diode parameters from forward current-voltage characteristics. *Appl. Phys. Lett.* **49,** 85–87 (1986).
23. Arora, K., Goel, N., Kumar, M. & Kumar, M. Ultrahigh Performance of Self-Powered β-Ga2O3 Thin Film Solar-Blind Photodetector Grown on Cost-Effective Si Substrate Using High-Temperature Seed Layer. *ACS Photonics* **5,** 2391–2401 (2018).
24. Mukhopadhyay, P. & Schoenfeld, W. V. High responsivity tin gallium oxide Schottky ultraviolet photodetectors. *J. Vac. Sci. Technol. A* **38,** 13403 (2020).
25. Guo, D. *et al.* Fabrication of β-Ga2O3 thin films and solar-blind photodetectors by laser MBE technology. *Opt. Mater. Express* **4,** 1067 (2014).
26. Lu, Y. M. *et al.* Preparation of Ga2O3 thin film solar-blind photodetectors based on mixed-phase structure by pulsed laser deposition. *Chinese Phys. B* **28,** (2019).
27. Zhao, B. *et al.* Solar-Blind Avalanche Photodetector Based On Single ZnO−Ga2O3 Core−Shell Microwire. (2015). doi:10.1021/acs.nanolett.5b00906
28. Dhar, S., Majumder, T., Chakraborty, P. & Mondal, S. P. DMSO modified PEDOT:PSS polymer/ZnO nanorods Schottky junction ultraviolet photodetector: Photoresponse, external quantum efficiency, detectivity, and responsivity augmentation using N doped graphene quantum dots. *Org. Electron. physics, Mater. Appl.* **53,** 101–110 (2018).
29. Nakagomi, S., Sakai, T., Kikuchi, K. & Kokubun, Y. β-Ga2O3/p-Type 4H-SiC Heterojunction Diodes and Applications to Deep-UV Photodiodes. *Phys. Status Solidi Appl. Mater. Sci.* **216,** 1–8 (2019).
30. Kong, W. Y. *et al.* Graphene-β-Ga2O3 heterojunction for highly sensitive deep UV photodetector application. *Adv. Mater.* **28,** 10725–10731 (2016).